Magnetoluminescence of self-assembled InP dots of various sizes

B. Kowalski*
Solid State Physics, Lund University, Box 118, 221 00 Lund, Sweden

S. Nomura
Solid State Physics, Lund University, Box 118, 221 00 Lund, Sweden
and The Institute of Physical and Chemical Research, Hirosawa 2-1, Wako-shi, Saitama, 351-0198, Japan

C. Pryor
Solid State Physics, Lund University, Box 118, 221 00 Lund, Sweden

Y. Aoyagi
Solid State Physics, Lund University, Box 118, 221 00 Lund, Sweden
and The Institute of Physical and Chemical Research, Hirosawa 2-1, Wako-shi, Saitama, 351-0198, Japan

N. Carlsson, M.-E. Pistol, P. Omling, L. Samuelson, and W. Seifert
Solid State Physics, Lund University, Box 118, 221 00 Lund, Sweden
(Received 5 January 1998)

We present photoluminescence measurements of self-assembled InP quantum dots on a GaAs surface (i.e., freestanding dots), under the influence of a high magnetic field. Reasonably sharp luminescence features are seen corresponding to the ground state, and several excited states. Magnetic-field-dependent measurements are presented and compared with calculations based on a finite-difference method using the envelope approximation. The calculations include a realistic pyramidal shape for the dots, as well as strain. We find good agreement between theory and experiments. [S0163-1829(98)01728-7]

I. INTRODUCTION

Quantum dots formed by Stranski-Krastanow growth mode have been explored for a number of material combinations.[1–3] The growth mechanism produces objects that exhibit strong electronic quantum confinement in all three directions. Spectroscopy of such quantum dots has been extensively developed to examine their electronic structure[4,5] and, in a few cases, effects of external perturbations.[6,7] An especially interesting modification to the environment of a quantum dot is the application of a strong magnetic field.[8–11] Just as the behavior of atoms in a magnetic field provided insight into atomic physics approximately 100 years ago, the application of a magnetic field to an ''artificial atom'' provides a method of elucidating the electronic structure of a quantum dot.

Such measurements are, however, hindered by the unavoidable sample inhomogeneities. Due to small fluctuations in the dot's size and shape, photoluminescence (PL) linewidths of 30–60 meV are seen in macroscopic measurements that average over an ensemble of Stranski-Krastanow dots. This linewidth is too large to distinguish luminescence features arising from the ground and excited states of the dots. At least some of the inhomogeneity arises from compositional inhomogeneities of the ternary buffer layer and may be reduced by using a binary alloy buffer layer, resulting in a reduced PL linewidth.[12] In addition to inhomogeneities, there may also be variation between growths. Both within-sample and between-sample variations make comparison with theory difficult since theoretical predictions depend critically on the shape and size of the dots. This is especially problematic when dealing with capped dots, since comparison with calculations requires assumptions about the dot geometry based on secondary samples left uncapped, or subjected to destructive electron microscopy.

To more directly compare theory and experiment, we have performed magnetic-field-dependent PL measurements on InP quantum dots that are deposited on a GaAs surface and left *uncapped*. Studying uncapped surface dots allows a more direct analysis since the exact geometry and size of the PL samples may be determined by atomic force microscopy (AFM). In this study we use these numbers as input parameters for the calculations that are based on a finite-difference method utilizing the envelope approximation and including strain and magnetic field. An accurate test of this theory is facilitated by varying the dot sizes between different samples that could be tuned by the growth temperature.[12] Our theoretical model realistically takes into account the low-symmetry pyramidal geometry. Consequently, we find lifting of degeneracies, as well as level anticrossings of energy eigenvalues as a function of magnetic field. These effects are seen in the experimental data.

We first present the experimental technique, followed by the magnetic-field-dependent PL measurements. The theoretical approach is then outlined, followed by a comparison with the experimental results.

II. EXPERIMENT

Free standing islands of InP on top of a [100] oriented GaAs buffer were grown by metalorganic vapor-phase epi-

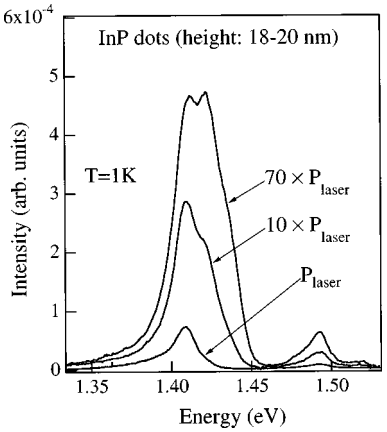

FIG. 1. Photoluminescence of InP dots on GaAs surface. Different laser excitation densities have been used.

taxy (MOVPE). The precursors were trimethylgallium, trimethylindium, arsine, and phosphine. The dots were left uncapped on the sample surface. Changing the deposition temperature gave different average dot sizes as measured with AFM. We measured two samples with dot heights of about 12–14 and 18–20 nm, grown at 580 and 610 °C, respectively. In addition to AFM measurements, the detailed geometrical shape of InP dots has been determined previously using high-resolution transmission electron microscopy (TEM).[13] The individual dots have the form of truncated pyramids, elongated along the [110] direction, defined by six side faces {111} and {110}. For the present samples the long and the short base diameter are within a range 60–85 and 40–60 nm, respectively, as deduced for known heights and formed facets as well as seen by TEM.

The PL measurements as a function of magnetic field B were conducted with a 300-mK ^{3}He system equipped with an 18-T solenoid superconducting magnet. The sample was immersed in pumped ^{3}He at a temperature of $T \approx 1$ K, and the optical access was by means of an optical fiber. The PL was excited by an Ar^+ laser operating at 488 nm, with typical powers of 0.1–10 mW before coupling into the fiber. Using different laser excitation power densities in PL the islands could be measured with or without state filling, i.e., population of excited states. The PL of the samples was dispersed with a $f/0.5$ m grating spectrometer and detected with a Ge photodiode cooled to 77 K. These measurements were performed with fixed orientations of the magnetic field parallel to the sample growth axis [001]. To clarify that the dot PL originates at the sample surface, 360-nm UV laser light was used to selectively excite the region close to the surface.

III. RESULTS

Figure 1 shows the spectrum for dots of 18–20 nm height using different laser excitation power densities. The PL from the InP dot samples at zero magnetic field consisted of features at 1.41–1.44 eV, as well as bulk GaAs acceptor and exciton related lines at 1.49 and 1.52 eV. The single line observed at 1.41 eV for low excitation power exhibits a full peak width at half-maximum (FWHM) of about 18 meV. With increasing power shoulders appear at higher energy that develop into peaks separated in energy by about 12 meV. The PL of InP Stranski-Krastanow dots can be attributed to excitonic transitions.[5] The peaks emerging with increasing excitation density can be assigned to state filling of excited states in the dots.[14] Such behavior is also observed for the dots of height in the range 12–14 nm. Here the peak separations amount to about 20 meV. The PL linewidths of the present InP dot samples grown on GaAs are smaller than InP surface dots on the $Ga_{0.5}In_{0.5}P$ buffer.[6] We attribute this to the absence of compositional inhomogeneities of the binary material combination as compared to the case of the ternary buffer layer.[12] To verify that the PL assigned to dots indeed originates at the surface, where the dots are, excitation with UV laser light was utilized. In this case, the lines related to GaAs bulk are strongly suppressed in contrast to the dot PL features.

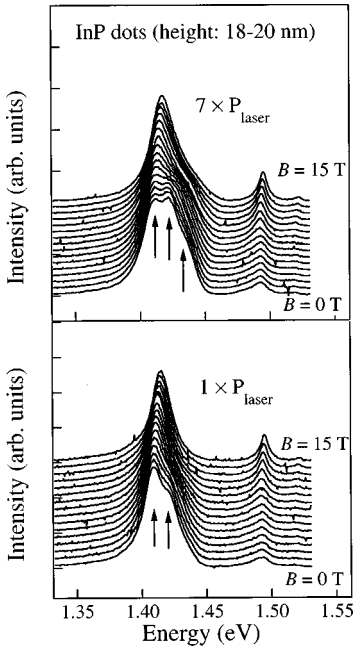

FIG. 2. Photoluminescence of InP dots (18–20-nm height) as a function of magnetic fields obtained for two different degrees of state filling.

When a magnetic field is applied the individual PL peaks shift. To exactly determine the position of each peak as a function of field the state-filling conditions were varied. It means that we first recorded the magnetic-field evolution of the lowest peak without state filling. Then the laser excitation power was increased to populate even the second level and to record its field evolution. Knowing the peak positions of the lowest peak the second peak could be fitted with higher accuracy. This procedure was repeated for the third PL peak, as is illustrated in Figs. 2(a) and 2(b) for the 18–20-nm-high dots. The peak positions were extracted using a Gaussian line profile. Shifts of the peak positions for the different laser excitation densities used here were not significant within the experimental accuracy. The lowest-energy PL peak showed a blueshift by about 6 meV as the field was increased from 0 to 15 T, whereas the next-higher peak redshifted by a little less than 4 meV. The highest-energy peak, which appears as a shoulder, redshifted up to 5 T, then blueshifted for $B > 5$ T. For the 12–14-nm dots a third peak was visible only for fields above 7 T. The peak positions as a

function of B are shown as circular symbols in Figs. 3(a) and 3(b) for the dot sizes 12–14 and 18–20 nm, respectively.

IV. THEORY

The observed PL spectra and their magnetic-field evolution provide a fingerprint of the electronic structure of these Stranski-Krastanow quantum dots. A proper theoretical treatment needs to take into account the geometry of the confining potential, which is given by both the heterostructure band offsets and the strain profile that modifies the band structure. The shape of the pyramids is shown in Fig. 4, as determined by AFM on these samples. This geometry is in agreement with earlier studies of InP dots.[13,15]

We calculated the strain profile and the electronic structure (in the envelope approximation) using a finite-difference method on a real-space mesh. This method has been successfully used to explain experimental results for InP Stranski-Krastanow dots embedded in $Ga_{0.5}In_{0.5}P$.[15–17] Continuum elastic theory is used to calculate the strain at each point of the mesh[15] with material dependent elastic constants taken from Ref. 18. The strain tensor e_{ij} $(i, j=x, y, z)$ was then used in the strain-dependent Hamiltonian. The later is written in Luttinger form for single particles and the magnetic field is included in the Landau gauge $\mathbf{A}=(0,Bx,0)$. The electron Hamiltonian is

$$H_e=\frac{m_0}{m_e}\left\{\frac{\hbar^2}{2m_0}[-\partial_{xx}^2-\partial_{yy}^2-\partial_{zz}^2]-i\,\frac{e\hbar B}{m_0c}\,\partial_y x+\frac{e^2B^2}{2m_0c^2}\,x^2\right\}+\frac{e\hbar B}{2m_0c}\,g^*s_z-a_c(e_{xx}+e_{yy}+e_{zz})+V_e. \tag{1}$$

The hole Hamiltonian is given by

$$H_h=T_h+H_h^{el}+V_h, \tag{2}$$

$$T_h=\begin{pmatrix} A_+ & D & C & 0\\ D^\dagger & A_- & 0 & C\\ C^\dagger & 0 & A_- & -D\\ 0 & C^\dagger & -D^\dagger & A_+\end{pmatrix},$$

$$A_\pm=\frac{\hbar^2}{2m_0}\left\{(\gamma_1\pm\gamma_2)(-\partial_{xx}^2-\partial_{yy}^2)-(\gamma_1\mp 2\gamma_2)\partial_{zz}^2+(\gamma_1\pm\gamma_2)\left[\frac{e\hbar B}{m_0c}\,i\partial_y x+\frac{e^2B^2}{2m_0c^2}\,x^2\right]\right\}-\frac{e\hbar B}{m_0c}\,\kappa j_z,$$

$$D=-i\,\frac{\hbar^2}{m_0}\sqrt{3}\partial_z(i\partial_x+\partial_y)-\frac{e\hbar B}{m_0c}\sqrt{3}\gamma_3\partial_z x,$$

$$C=-\frac{\hbar^2}{2m_0}\sqrt{3}[\gamma_2(-\partial_{xx}^2+\partial_{yy}^2)+2i\gamma_3\partial_x\partial_y]-\sqrt{3}\,\frac{e\hbar B}{m_0c}x\left[\gamma_3\left(\partial_x+\frac{1}{2}\right)-i\gamma_2\partial_y\right]+\frac{\sqrt{3}}{2}\,\gamma_2\,\frac{e^2B^2}{m_0c^2}\,x^2,$$

$$H_h^{el}=-a(e_{xx}+e_{yy}+e_{zz})\mathbf{I}-3b\left[\left(L_x^2-\frac{1}{3}\,L^2\right)e_{xx}+\text{c.p.}\right]-\sqrt{3}d[(L_xL_y+L_yL_x)e_{xy}+\text{c.p.}].$$

Here m_0 is the free-electron mass. m^* and g^* are the effective mass and effective g value of the conduction band, respectively, γ_1, γ_2, γ_3, and κ are the Luttinger valence-band parameters, and a_c, a, b, and d are deformation potentials. The parameters relevant for the two materials are taken from Ref. 18. $V_{e,h}$ are the local band edges (without strain) for electrons and holes. Here a valence-band offset of 340 meV between unstrained InP and GaAs has been used. This is based on transition-metal impurity spectra.[18] For the present study we did the numerical modeling for two different dot heights of 13 and 19 nm of the InP dots on a GaAs surface, corresponding to the two sizes of quantum dots that were investigated experimentally.

Figures 3(a) and 3(b) show the calculated magnetic-field dependencies of the conduction-electron states for 13- and 19-nm-high InP dots, respectively. The reference energy in each of the two calculations has been adjusted to fit the lowest PL transition energy at $B=0$ T, in order to facilitate comparison with the experiments. The levels appear as doublets due to the inclusion of spin in the Hamiltonian. Comparing the two dot sizes at zero field, we see larger energy splittings for the smaller dots, as expected. With increasing magnetic field the ground state shifts to higher energy for both dot sizes. The second level decreases in energy for fields up to 15 T, and then increases. The third and fourth levels show an anticrossing at $B=7$ and 13 T, for the larger and smaller dots, respectively. For both dot sizes the experimentally observed evolution of the PL peaks with field is reproduced by the calculation. The level structure becomes more complicated for higher-lying levels.

While the agreement between experiment and theory looks very good, some insights and a qualitative explanation may be obtained by approximating the pyramidal quantum dots by a rotationally symmetric structure. The different electronic states can then be characterized by an angular momentum l $(l\approx 0,\pm 1,\pm 2...)$, that interacts paramagnetically

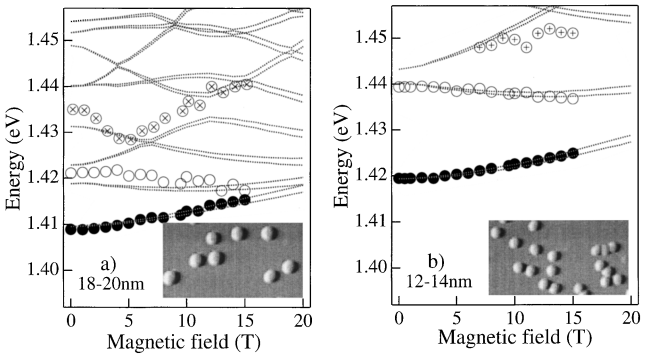

FIG. 3. The peak energies as a function of magnetic field for two different dot sizes, corresponding to a dot height of 18–20 nm (a) and 12–14 nm (b). The dashed lines correspond to a calculation (see text). The insets show AFM images of 0.9×0.5-μm fields.

with the magnetic field. Depending on the sign of l the levels shift to lower or higher energy with increasing magnetic field. In this picture, levels with different l would then give the main contribution to the field evolution of the various PL features. The lowest peak is related to levels with $l\approx0$. The two subsequent levels at higher energy have $l\approx-1$ and $l\approx+1$, in this order.

At the same time, we can see the effect of the irregular potential geometry in our realistic calculation. For instance, the levels with $l\approx-1$ and $l\approx+1$ are not degenerate at zero magnetic field, as would be the case for rotational symmetry. Furthermore, the lower symmetry induces anticrossings of two levels as a function of magnetic field, see, e.g., Fig. 3(a) at $B=7$ or 11 T. For this we indeed find some manifestation in the experimental data. Regarding the dots with 18–20-nm height, see Fig. 3(a), there is a peculiarity in the highest energy peak. Its shift with field changes direction, which can be explained by a level with $l\approx-2$. At $B=5$ T the redshifting level with $l\approx-2$ exhibits an apparent anticrossing with the $l\approx+1$ level. However, a corresponding experimental PL peak at lower energy for higher fields is not visible, probably because it is not resolved.

It should be noted that the calculations presented in Figs. 3(a) and 3(b) do not include the influence of the magnetic field on the holes. This is justified by the fact that the hole effective mass is considerably larger than the electron effective mass, making the energy shifts with field much smaller for holes than for the electrons. In fact, our theoretical model, when applied on the holes, gives level spacings and shifts with magnetic field (0–15 T) that are of the order of 1–2 meV. Moreover, it can be assumed that the imperfections and inhomogeneities responsible for the line broadening allow optical transition between a particular electron state and several hole states.[15] The quite low symmetry of the dots related to the irregular potential and strain field may also play a role. Thus, the holes contribute primarily to the spectral broadening. The agreement of the calculations for the electrons with the experiments implies that the main contribution to the magnetic-field-dependent spectra stems from the electrons in the InP/GaAs dots.

It is not clear, however, that both the electrons and holes are confined in the InP dot on GaAs. The holes could be localized in the GaAs underneath the dot. The calculation indeed suggests such a type-II line-up of the valence- and conduction-band edges (Fig. 4). This suggests an optical recombination energy of approximately 1.2–1.3 eV, in contrast to the experimental findings. A possible explanation could be to have holes and electrons recombining in the strained GaAs. This could perhaps explain the recombination energy found to be approximately 1.4 eV. However, theory does not suggest a barrier that would keep the electrons out of the dot. We therefore consider this scenario to be unlikely. On the other hand, it can be speculated whether the recombination might involve holes bound to an acceptor in the InP dots.[19] In any case the main contribution to the magnetic-field dependence of the experimental PL spectra originates from the electrons. Furthermore, the experimental results for varying sizes of the quantum dots are well explained by the model.

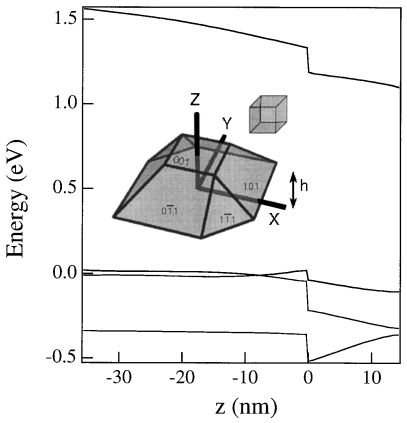

FIG. 4. Conduction- and valence-band edges along the z axis through the center of the dot. The GaAs surface is at zero and the dot rests on top (positive z). The inset shows the dot geometry: it has the form of a truncated pyramid (perspective and top view).

V. CONCLUSIONS

The magneto-PL of the ground and excited levels in free-standing Stranski-Krastanow InP quantum dots of different sizes has been studied. Different state filling conditions were employed to follow the magnetic field evolution of the levels to allow for higher accuracy. For the PL features pronounced shifts with magnetic field were found that agree well with a realistic calculation. The model takes into account the complex strain profile corresponding to the pyramidal dot shape, and the dot sizes as obtained by structural investigations on the very same samples. Some indication for the predicted anticrossings induced by the irregular shape were found experimentally.

ACKNOWLEDGMENTS

This work has been financed by the Swedish Natural Science Research Council, Swedish Research Council for Engineering Science, NUTEK, and the Göran Gustafsson Foundation for Research in Natural Sciences and Medicine. One of the authors (S.N.) would like to acknowledge support from the Computation Center at RIKEN for using a Fujitsu VPP-500, and from the Ministry of Education, Science, Sports and Culture of Japan by a Grant-in-Aid for Scientific Research.

*Electronic address: bernhard.kowalski@ftf.lth.se

[1] N. Carlsson, K. Georgsson, L. Montelius, L. Samuelson, W. Seifert, and R. Wallenberg, J. Cryst. Growth **156**, 23 (1995).

[2] J. M. Moison, F. Houzay, F. Barthe, L. Leprince, E. Andre, and O. Vatel, Appl. Phys. Lett. **64**, 196 (1994).

[3] M. S. Miller, J. O. Malm, M. E. Pistol, S. Jeppesen, B. Kowalski, K. Georgsson, and L. Samuelson, J. Appl. Phys. **80**, 3360 (1996).

[4] J. Y. Marzin, J. M. Gerard, A. Izraël, D. Barrier, and G. Bastard, Phys. Rev. Lett. **73**, 716 (1994).

[5] D. Hessman, P. Castrillo, M.-E. Pistol, C. Pryor, and L. Samuelson, Appl. Phys. Lett. **69**, 749 (1996).

[6] M.-E. Pistol, N. Carlsson, C. Persson, W. Seifert, and L. Samuelson, Appl. Phys. Lett. **67**, 1438 (1995).

[7] I. E. Itskevich, M. Henini, H. A. Carmona, L. Eaves, and P. C. Main, Appl. Phys. Lett. **70**, 505 (1997).

[8] D. Heitmann, in *Confined Electrons and Photons*, edited by E. Burstein and C. Weisbuch (Plenum, New York, 1995), Vol. 340, p. 305.

[9] M. Bayer, A. Schmidt, A. Forchel, F. Faller, T. L. Reinecke, P. A. Knipp, A. A. Dremin, and V. D. Kulakovskii, Phys. Rev. Lett. **74**, 3439 (1995).

[10] R. Rinaldi, P. V. Giugno, R. Cingolani, H. Lipsanen, M. Sopanen, J. Tulkki, and J. Ahopelto, Phys. Rev. Lett. **77**, 342 (1996).

[11] U. Bockelmann, W. Heller, and G. Abstreiter, Phys. Rev. B **55**, 4469 (1997).

[12] W. Seifert, N. Carlsson, J. Johansson, M.-E. Pistol, and L. Samuelson, J. Cryst. Growth **170**, 39 (1997).

[13] K. Georgsson, N. Carlsson, L. Samuelson, and W. Seifert, Appl. Phys. Lett. **67**, 2981 (1995).

[14] P. Castrillo, D. Hessman, M. E. Pistol, S. Anand, N. Carlsson, L. Samuelson, and W. Seifert, Appl. Phys. Lett. **67**, 1905 (1995).

[15] C. Pryor, M.-E. Pistol, and L. Samuelson, Phys. Rev. B **56**, 10404 (1997).

[16] L. Samuelson, S. Anand, N. Carlsson, P. Castrillo, K. Georgsson, L. Wallenberg, A. Carlsson, J. O. Bovin, S. Nomura, Y. Aoyagi, T. Sugano, K. Uchida, and N. Miura, in *23rd International Conference on the Physics of Semiconductors*, edited by M. Scheffler, (World Scientific, Singapore, 1996), p. 1269.

[17] S. Nomura, L. Samuelson, C. Pryor, M.-E. Pistol, K. Uchida, N. Miura, T. Sugano, and Y. Aoyagi, Appl. Phys. Lett. **71**, 2316 (1997).

[18] *Semiconductors*, edited by O. Madelung, M. Schulz, and H. Weiss, Landolt-Börnstein, New Series, Group III, Vol. 17, pt. a (Springer-Verlag, Berlin, 1982).

[19] M.-E. Pistol, J. O. Bovin, A. Carlsson, N. Carlsson, P. Castrillo, K. Georgsson, D. Hessman, T. Junno, L. Montelius, C. Persson, L. Samuelson, W. Seifert, and L. Wallenberg, in *23rd International Conference on the Physics of Semiconductors*, edited by M. Scheffler (World Scientific, Singapore, 1996), p. 1317.